Article

Computational Search for New W−Mo−B Compounds

Alexander G. Kvashnin,* Christian Tantardini,* Hayk A. Zakaryan, Yulia A. Kvashnina, and Artem R. Oganov
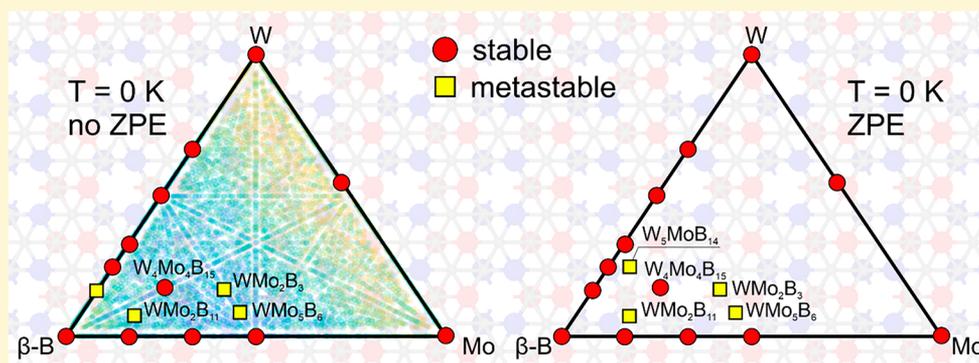
Read Online

ACCESS | 📊 Metrics & More | 📰 Article Recommendations | 🆂🅸 Supporting Information

ABSTRACT: Crystal structure prediction of new ternary compounds is challenging due to a very large chemical space with many possible compositions, few of which turn out to be stable. Using the evolutionary algorithm USPEX, here we predicted potentially superhard ternary compounds in the W−Mo−B system. Five new stable ternary compounds with various chemical compositions were predicted at different temperatures, and the composition−temperature phase diagrams were calculated. Electronic properties of the new compounds were studied in detail to find their correlation with the mechanical properties, crystal structure, and atomic composition (i.e., mass percentage of elements within the molecular formula).

INTRODUCTION

During the past decades, the problem of crystal structure prediction was efficiently solved by many different approaches[1] including USPEX[2−4] (evolutionary algorithm), CALYPSO[5] (particle swarm optimization), AIRSS[6,7] (random structure searching), XtalOpt[8] (evolutionary algorithm), etc. The combination of structure searching algorithms with first-principles or semiempirical calculations makes it possible to find novel stable structures and/or compositions.[1] But only USPEX is robust enough to be employed with success for both inorganic and organic materials.[1] A noteworthy feature of USPEX is the ability to predict crystal structures (unary, binary, ternary, etc.) that have not only a specific chemical composition but also desired physical properties by using multiobjective optimization.[9]

USPEX has been widely applied to the prediction of binary hard and superhard compounds (i.e., those with Vickers hardness > 40 GPa[5−7]) such as metal borides, carbides, nitrides, and the like.[8−22,28−32] Apart from their high hardness, these materials are also known for a combination of outstanding physical properties: electrical conductivity, low compressibility, high melting temperature, and high shear strength.[23−32] Some physical properties of binary compounds, such as hardness for metal borides, could be further improved by adding a third element: an addition of 3 atom % of Mo to

"WB₄" (now it is established[33] that this phase is WB_{5-x} with typical $x \sim 0.7−0.8$) leads to a 15% increase in Vickers hardness, from 28.1 ± 1.4 to 33.4 ± 0.9 GPa when the applied load is 4.90 N.[34,35] Furthermore, varying the W:Mo ratio may lead to the formation of new ternary structures, with unknown structural motifs and with mechanical properties exceeding those of the pristine and doped binary compounds. Thus, the prediction of the crystal structure of ternary compounds becomes fundamentally important for new hard and superhard materials.

METHOD AND COMPUTATIONAL DETAILS

An efficient prediction of ternary W−Mo−B compounds was achieved using the evolutionary algorithm USPEX.[2−4] To make the prediction as accurate as possible, we used a multistep procedure consisting of (i) the collection of all possible information about binary compounds (the edges of a triangular phase diagram) from literature and a variable-composition evolutionary search for binary compounds; (ii) a
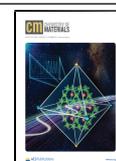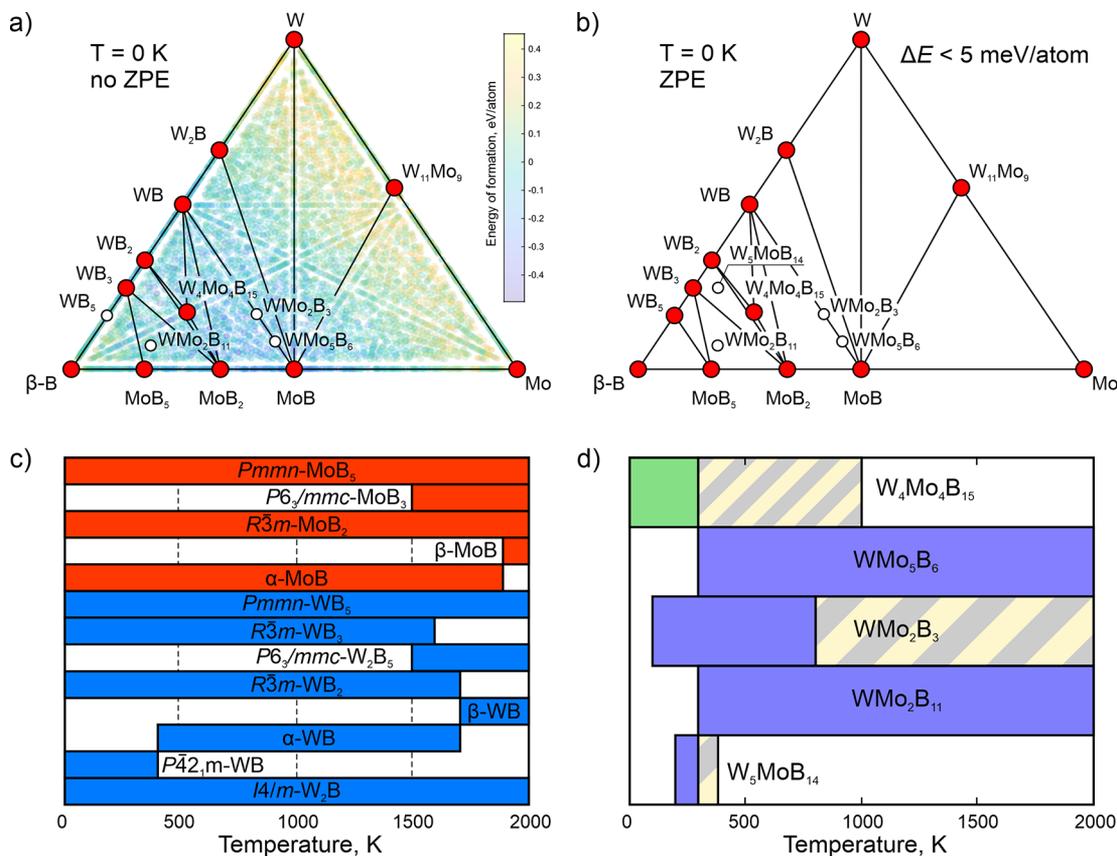
Figure 1. (a) Ternary phase diagram of the W−Mo−B system at 0 K (no ZPE contribution). (b) Ternary phase diagram showing metastable ternary phases with ΔE < 5 meV/atom, with ZPE. Stable and metastable structures are shown by red and white circles, respectively. Red dots indicate individual structures. (c) Composition−temperature diagram for binary phases in the W−B and Mo− B systems calculated using the quasi-harmonic approximation. (d) Composition−temperature diagram for the predicted ternary compounds showing the possibility of experimental synthesis at high-temperature conditions. Green color represents the stable structure at 0 K, blue bars are metastable structures at 0 K, and shaded areas show the stability regions calculated when taking configurational entropy contribution into account.

variable-composition evolutionary search for ternary compounds, without any restrictions except for the number of atoms in the primitive cell (≤48 atoms); (iii) a variable-composition evolutionary search for ternary compounds with seeds that consisted of all known unary, binary, and ternary compounds; and (iv) an evolutionary search along pseudobinary joins from (ii) and (iii). Step (i) enabled the prediction of all structures of binary compounds necessary for step (iii), whereas step (ii) made it possible to find all stable and metastable structures for ternary compounds that do not have the same crystal structure types as binary compounds.

During the structure search, the first generation of 350 structures was produced randomly with up to 48 atoms in the primitive cell. Each subsequent generation consisting of 250 structures was produced by applying the heredity (40% of each generation), softmutation (20%), and transmutation (20%) operators; 20% of each generation was produced using random symmetric[4] and random topological generators.[36] Stable binary compounds in the W−B and Mo−B systems for step (iii) were taken from refs 14 and 15 and ref 26, respectively. Additional searches for stable structures were performed for the WMo-B and WB−MoB systems, where the first generation of the structure candidates contained 150 structures with up to 48 atoms in the primitive cell, while succeeding generations contained 100 structures.

Structure relaxations and total energy calculations were performed using the projector augmented-wave (PAW) method[37,38] and the generalized gradient approximation (GGA) using the Perdew−Burke−Ernzerhof (PBE) exchange-correlation density functional as implemented in the VASP package.[38−41] The PAW potentials with 12, 6, and 3 valence electrons for molybdenum, tungsten, and boron were used to describe the electron−ion interactions. Crystal structures were

relaxed until the maximum net force on atoms became less than 0.01 eV/Å. The plane wave energy cutoff of 500 eV and Methfessel−Paxton[42] smearing of electronic occupations ensured the convergence of total energies. The Γ-centered k-point meshes of 9 × 7 × 7 (W_4MoB_{15}), 10 × 10 × 6 (W_5MoB_{14}), 3 × 17 × 17 (WMo_2B_{11}), 8 × 8 × 10 (WMo_2B_3), and 10 × 14 × 5 (WMo_5B_6) were used for Brillouin zone sampling. After relaxing the crystal structure, we applied strains of +1% and −1% and extracted the elastic constants from stress−strain relations. The crystal structures were visualized using VESTA software.[43]

We have computed the Helmholtz free energy as

$$F(T) = E_0(V) + F_{vib}(V, T) \tag{1}$$

where E_0 is the total energy from the DFT calculations and F_{vib} is vibrational Helmholtz free energy calculated from the following relation in the quasiharmonic approximation:[44]

$$F_{vib}(V, T) = k_B T \int g(\omega(V)) \ln\left[1 - \exp\left(-\frac{\hbar\omega(V)}{k_B T}\right)\right] d\omega$$
$$+ \frac{1}{2} \int g(\omega(V))\hbar\omega \, d\omega \tag{2}$$

The first term represents vibrational energy, while the second one is the zero-point energy; $g(\omega(V))$ is the phonon density of states at the given volume, calculated by the finite displacements method as implemented in PHONOPY,[45,46] using forces computed by VASP.[47−49]

The Vickers hardness H_V and fracture toughness K_{IC} were estimated using the empirical Mazhnik−Oganov[50] model:

$$H_V = \gamma_0 \chi(\nu) E \tag{3}$$

where $\gamma_0 = 0.096$, $\chi(\nu)$ is a dimensionless function of Poisson's ratio, and E is Young's modulus:[50]

$$\chi(\nu) = \frac{1 - 8.5\nu + 19.5\nu^2}{1 - 7.5\nu + 12.2\nu^2 + 19.6\nu^3} \tag{4}$$

The fracture toughness was calculated as[50]

$$K_{IC} = \alpha_0^{-1/2} \cdot V_0^{1/6} \cdot [\zeta(\nu)E]^{3/2} \tag{5}$$

where α_0 depends on the chemical bonding in the material and has the units of pressure, V_0 is the volume per atom, and $\zeta(\nu)$ is a dimensionless function of Poisson's ratio:

$$\zeta(\nu) = \frac{1 - 13.7\nu + 48.6\nu^2}{1 - 15.2\nu + 70.2\nu^2 - 81.5\nu^3} \tag{6}$$

Test calculations for several materials show good agreement with the reference experimental data: the calculated values of the Vickers hardness are, for diamond, 99 GPa (experimental value ∼ 96 GPa),[51] for TiN, 21 GPa (20.5 GPa),[52] and for c-BN, 71 GPa (∼66 GPa).[53]

■ RESULTS AND DISCUSSION

Stability. The data obtained from the USPEX evolutionary searches of binary and ternary compounds enabled diagramming a three-dimensional convex hull at 0 K (Figure 1a). We predicted all known stable binary compounds in agreement with the previous investigations.[14,23,25,26,54] The crystal structure of pure boron should be taken into account to calculate the energies of formation (or Gibbs free energies of formation at finite temperature) of each W−Mo−B compound. It has been shown in previous experimental and theoretical works[55−60] that α- and β-boron are isenthalpic at 0 K, whereas at ∼2000 K the energy difference of these phases reaches 20 meV/atom,[60] which may significantly change the entire convex hull of a ternary system at higher temperatures. As the structure of β-B is disordered and the lowest-energy model $hR1280$ contains 1280 atoms[61] with the energy 7.5 meV/atoms lower than α-B at 0 K, we used the recently predicted β-B$_{106}$ (2 meV/atom lower than α-B including ZPE). In this work, we did all calculations (including phonon calculations) on the 106-atom β-B$_{106}$ model and applied a constant correction for the energy difference between $hR1280$ and β-B$_{106}$. The configurational entropy of β-boron to the Gibbs free energy, estimated by Ogitsu et al.[62] using thermodynamic integration from the high-temperature limit, does not exceed 0.28 J/mol at 2000 K. Such values can be neglected in our calculations at much lower temperatures because the vibrational contribution is much higher in this case.

Among other tungsten monoborides in the W−B edge of the three-dimensional convex hull, $P\bar{4}2_1m$-WB is found to be thermodynamically stable at 0 K, in agreement with previous studies.[14,27] The highest tungsten boride WB$_5$ is predicted to be metastable at 0 K (Figure 1a), in agreement with our previous work.[14] When the zero-point energy (ZPE) contribution is taken into account for thermodynamically stable and metastable compounds, WB$_5$ becomes thermodynamically stable (Figure 1b). Several metastable ternary compounds with the distance from the convex hull smaller than 5 meV/atom, shown by white circles in Figure 1b, could potentially be experimentally obtained at high-temperature conditions.

Five new ternary compounds were predicted: W$_4$Mo$_4$B$_{15}$, WMo$_5$B$_6$, WMo$_2$B$_3$, WMo$_2$B$_{11}$, and W$_5$MoB$_{14}$ (Figure 1). The

enthalpies of formation of the predicted phases at 0 K are −0.41, −0.47, −0.45, −0.26, and −0.32 eV/atom (0, 2.5, 4.1, 5.2, and 5.1 meV/atom above the convex hull, with ZPE included). The ZPE data are listed in Supporting Information Table S1.

Changes in pressure and temperature could lead to the stabilization of new compounds. Thus, we calculated the Gibbs free energy of formation for all predicted compounds within the quasi-harmonic approximation and constructed the composition−temperature diagrams (Figure 1c, d) (the phonon densities of states are shown in Supporting Information Figure S4). The stability ranges of the W−B phases are consistent with our previous study[14] (Figure 1c). We found that $P6_3/mmc$-W$_2$B$_5$, proposed by Cheng et al.,[25] becomes thermodynamically stable at ∼1700 K, expelling both WB$_3$ and WB$_2$ from the phase diagram (Figure 1c).

Here we studied only the stoichiometric structures of the highest metal borides, WB$_5$ and MoB$_5$, whereas recent works[26,33] showed the stabilization of the disordered structures WB$_{4.2}$ and MoB$_{4.7}$ at higher temperatures. However, representing these phases as WB$_5$ and MoB$_5$ in the calculated ternary convex hull will not influence the stability of the predicted ternary compounds.

The temperature stability of predicted ternary compounds was calculated both with (shaded areas in Figure 1d) and without (Figure 1d) taking into account the configurational entropy. Among these compounds, only W$_4$Mo$_4$B$_{15}$ is stable at 0 K (Figure 1a,d), but in a very narrow stability field, from 0 to 300 K, limiting the possibility to synthesize it. However, its stability field is significantly expanded (up to 1000 K) by considering the contribution from configurational entropy (shaded area in Figure 1d). All five predicted ternary compounds potentially have high configurational entropy due to the formation of solid solutions. As molybdenum and tungsten atoms have similar sizes, electronegativities, and electronic configurations, different patterns of ordering of W and Mo atoms in a ternary compound will not significantly change the energy of the system. Considering that all possible configurations have similar energies, we estimated configurational entropy of each ternary compound using the upper bound for the configurational entropy of a Mo$_x$W$_{1−x}$B solid solution which is $S_{conf} = k_B(x \ln(x) + (1−x) \ln(1−x))$. Calculated values for different temperatures are shown in the Supporting Information (Table S2). One can see that configurational entropy expands the stability range of the WMo$_2$B$_3$ compound up to 2000 K, while without configurational entropy this compound was predicted to be stable up to 800 K. This increase of the stability field comes from the largest configurational entropy of WMo$_2$B$_3$ compared to other ternary compounds (see Table S2). Thus, three predicted ternary compounds, WMo$_2$B$_3$, WMo$_5$B$_6$, and WMo$_2$B$_{11}$, which have not been predicted to be thermodynamically stable at 0 K, could be potentially synthesized at high-temperature conditions and are stable from 300 to at least 2000 K. As WMo$_2$B$_3$ and WMo$_5$B$_6$ have similar structure types (α-MoB) but with different W/Mo ratios, they will merge into a single WB−MoB solid solution at high temperatures.

Crystal Structures. The crystal structures of some of the predicted ternary compounds are similar to those of binary compounds, and these ternary compounds can be obtained by substituting one element with another in the binary structure. The other predicted ternary compounds are derivatives of the already known structural types of binary compounds.

Predicted Pm-W$_4$Mo$_4$B$_{15}$ can be considered a derivative of the MoB$_2$-type structure, but having the AA stacking of the $P6_3/mmc$-MoB$_2$ layers with 1/2 of the Mo atoms in the unit cell replaced by the W atoms. The hexagonal layer of boron is lacking an atom if compared to the ideal structure of the boron sublattice in $P6_3/mmc$-MoB$_2$ (Supporting Information Figure S1).

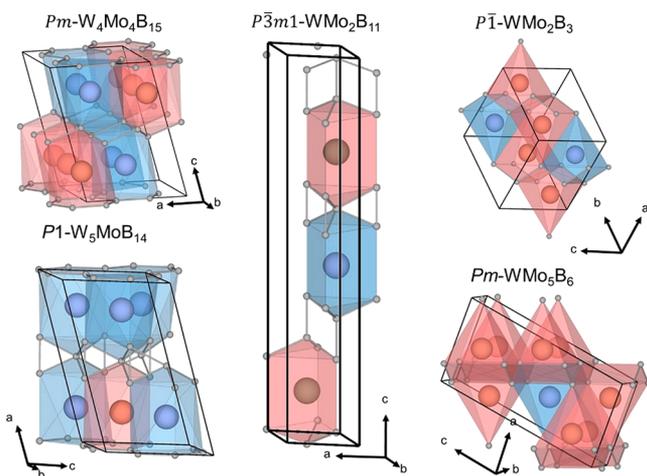$P1$-W$_5$MoB$_{14}$, found using the variable-composition evolutionary search (Figure 2), is an experimentally and

Figure 2. Crystal structures of the predicted ternary compounds W$_x$Mo$_y$B$_z$: red spheres, molybdenum; blue spheres, tungsten; gray spheres, boron atoms.

theoretically previously unknown crystal structure type. A comparison with the well-known crystal structures of binary compounds shows that it is a derivative of $P6_3/mmc$-MoB$_2$ characterized by one vacancy in the honeycomb boron layer and three additional boron atoms located on top of the boron atom in the Wyckoff position 24i of $P6_3/mmc$-MoB$_2$ (Supporting Information Figure S2).

Predicted $P\bar{3}m1$-WMo$_2$B$_{11}$ can be viewed as a layered structure with two alternating types of layers, one of which has an MoB$_4$-type structure (Figure 2 and Supporting Information Figure S3); MoB$_4$ is a hypothetical structure[23] that has never been found in experiments.[26,63] The second type of layers in WMo$_2$B$_{11}$ has the same structure as the modified MoB$_2$-type layers in $P1$-W$_5$MoB$_{14}$. Because of the presence of structural motifs from very hard compounds, WMo$_2$B$_{11}$ is expected to have similarly high mechanical characteristics (e.g., the Vickers hardness) as its hypothetical binary analogues.[23]

Pm-WMo$_5$B$_6$ and $P\bar{1}$-WMo$_2$B$_3$ belong to the well-known α-MoB crystal type with some of the Mo atoms substituted by the W atoms. Having the same crystal type, these structures may in fact be representatives of a continuous solid solution as shown below. The different doping ratios of α-MoB by tungsten in these two structures can potentially mean different mechanical properties.

Electronic Properties. The thermodynamic stability of a crystal is related to the presence of defects, which in small quantities can lower the energy of a crystal to its ground state. Such defects as substitutions or vacancies affect also the electronic properties with consequences on charge and heat transports. The evolutionary algorithm USPEX allowed us to predict three new ternary structures without full analogues among binary compounds: W$_4$Mo$_4$B$_{15}$, W$_5$MoB$_{14}$, and WMo$_2$B$_{11}$. Thus, we are interested in understanding how the different concentrations of Mo and W expressed as atomic percentage (W/Mo%) in the chemical formula affect the conductivities of these structures looking at valence and conduction bands at the Fermi level.[64] Such an investigation can be performed through an analysis of the projected density of states (PDOS).[52−54] The PDOS shows the relative contribution of each atom coming from different types of orbitals to the density of states.

In W$_4$Mo$_4$B$_{15}$ Mo and W atoms are at the same concentration, and they have d-orbitals equally populated at the Fermi level giving the metallic behavior at the structure
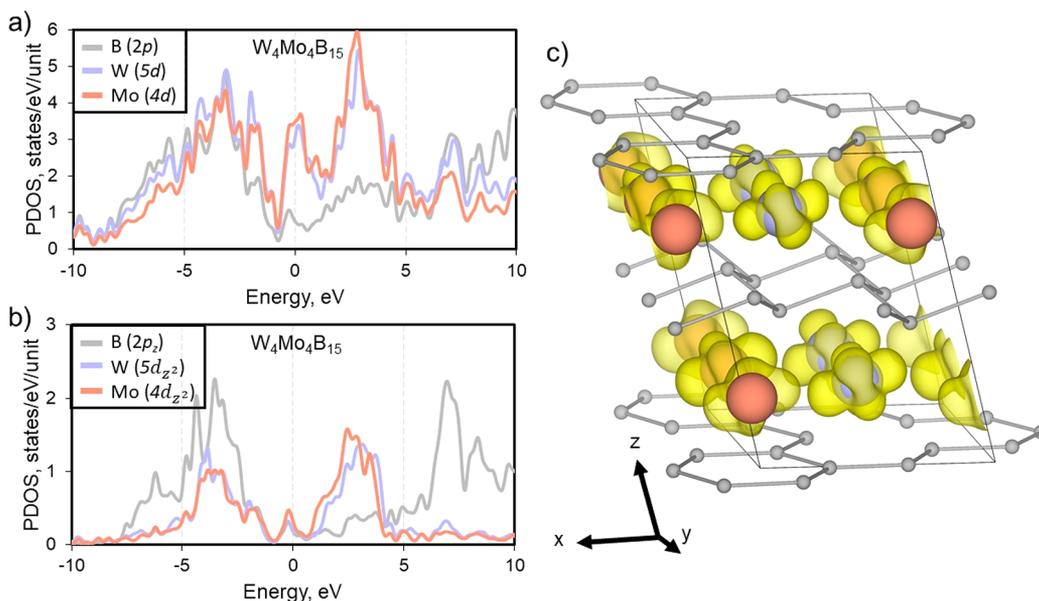

Figure 3. Projected densities of states of (a, b) W$_4$Mo$_4$B$_{15}$: gray, boron; red, molybdenum; blue, tungsten. (c) Electron density of W$_4$Mo$_4$B$_{15}$ plotted in the range from E_F −0.5 to E_F +0.5 eV. The isosurface value is 0.01 e/Å^3. Red spheres, molybdenum; blue spheres, tungsten; gray spheres, boron atoms.
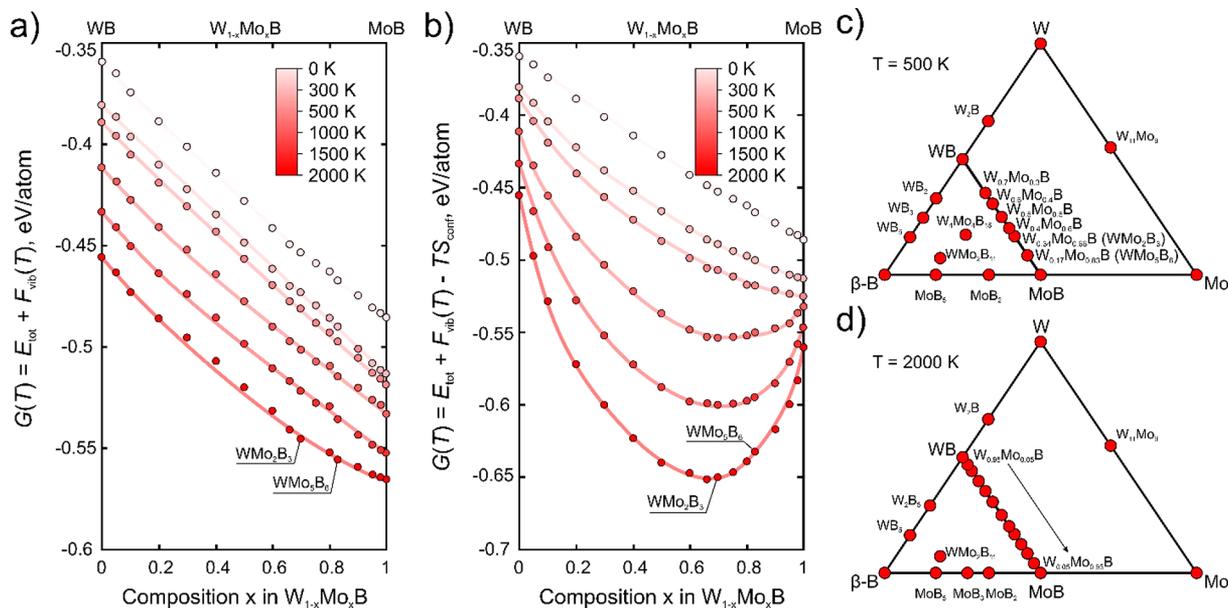
Figure 4. Gibbs free energies of formation calculated for WB−MoB solid solutions ($W_{1-x}Mo_xB$ phases) (a) without and (b) with contribution from configurational entropy. Ternary convex hull that included considered WB−MoB solid solutions at (c) 500 and (d) 2000 K. Stable structures are shown by red circles.

Table 1. Calculated Bulk Modulus (K), Shear Modulus (G), Young's Modulus (E), Poisson's Ratio (v), Vickers Hardness (H_V), and Fracture Toughness (K_{IC}) for the Predicted Ternary Compounds WMo_2B_{11}, W_5MoB_{14}, $W_4Mo_4B_{15}$, WMo_2B_3, and WMo_5B_6 in Comparison with Those of α-WB, α-MoB, $P6_3/mmc$-MoB_2, and $P6_3/mmc$-MoB_4

property	WMo_2B_{11}	W_5MoB_{14}	$W_4Mo_4B_{15}$	WMo_2B_3	WMo_5B_6	α-WB	α-MoB	$P6_3/mmc$-MoB_2	$P6_3/mmc$-MoB_4
K, GPa	224	301	311	306	319	349	308	310	285
G, GPa	191	235	241	185	198	192	203	237	211
E, GPa	448	559	575	461	492	486	499	566	507
v	0.167	0.191	0.193	0.249	0.243	0.27	0.229	0.195	0.203
H_V, GPa	29.7	31.9	32.2	21.4	22.7	23.5[b]	23.2[a]	31.1[a]	15.6
K_{IC}, MPa·m$^{0.5}$	3.01	4.38	4.61	3.97	4.28	4.6	4.22	4.51	1.74

[a]The experimental H_V values of α-MoB and $P6_3/mmc$-MoB_2 are 23.0[54] and 24.2 GPa,[65] respectively. [b]The experimental H_V value of α-WB is 25.3 GPa.[66]

(Figure 3a). Anionic vacancies (V_A^0) are present within boron layers of $W_4Mo_4B_{15}$, which act as electron donors.

$$V_A^0 \rightleftharpoons V_A^\bullet + e'$$
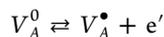
These extra electrons make the conductivity along the z-axis much lower than along other directions, as confirmed by the plot of the charge density corresponding to bands at the Fermi level: this density has clear 2D character (Figure 3c). Thus, the newly predicted compound $W_4Mo_4B_{15}$ could be employed for the future development of directional conductors having good in-plane conductivity.

Both W_5MoB_{14} and WMo_2B_{11} are seen to have metallic behavior with the predominant contribution to the Fermi level from the metallic species in excess with respect to the other (see Supporting Information, Figure S5).

Stability of the $W_{1-x}Mo_xB$ Phases. It is interesting to see how the thermodynamic stability of ternary compounds obtained by the doping of binary ones is correlated with the chemical composition of the stoichiometric unit expressed as a mass ratio. This correlation is useful to determine the extent to which a binary compound can be doped without losing stability and how the properties of the obtained ternary compounds change depending on whether their binary analogues are Mo- or W-rich. WMo_5B_6 and WMo_2B_3 both

have the α-MoB-type structure (Figure 2). To enrich the study of the thermodynamic stability of these phases we examined the stabilities of solid solutions made of various concentrations of W atoms in the α-MoB structure. We constructed 15 more structures corresponding to $W_{1-x}Mo_xB$ ($x = 0, 0.1, ..., 1$) compositions and calculated their Gibbs free energies of formation with and without taking into account the configurational entropy (see Figure 4a,b). Convex dependencies of the Gibbs free energy of formation for $W_{1-x}Mo_xB$ phases will lead to stabilization of many of intermediate compositions. For these phases configurational entropy plays a crucial role in the stability which can be clearly seen from Figure 4c,d. Even at 500 K, the $W_{1-x}Mo_xB$ solid solutions with $x = 0.3, 0.4, 0.5,$ and 0.6 become stable. A temperature increase (2000 K) leads to further stabilization of almost all compositions along the WB−MoB edge of the convex hull (Figure 4d).

These structures are created by adding substitutional defects to the α-MoB structure, where the W atoms replace some of the Mo atoms, potentially enhancing the mechanical properties. The structures like $W_4Mo_4B_{15}$, W_5MoB_{14}, and WMo_2B_{11}, which have no counterparts in the known binary compounds, are derivatives of the MoB_z structures with some W replacing Mo and with boron vacancies. Thus, ternary borides may be

considered as another type of material forming the basis of high-entropy alloys.

Mechanical Properties. It is known from the literature that molybdenum monoborides do not have extremely high mechanical characteristics, i.e., hardness. For WMo_5B_6 and WMo_2B_3, the addition of tungsten impurities to α-MoB did not lead to a significant change in the mechanical characteristics (Table 1). The calculations of the elastic and mechanical parameters were performed for all ternary compounds predicted in this study, including higher borides. The Vickers hardness and fracture toughness were calculated using the Mazhnik—Oganov model.[50] In this way, in the ternary system we predicted a new stable compound ($W_4Mo_4B_{15}$) with very good mechanical properties: the Vickers hardness is 32 GPa, and fracture toughness is 4.6 MPa·m$^{0.5}$.

Unusually, higher electronic delocalization of $W_4Mo_4B_{15}$, W_5MoB_{14}, and WMo_2B_{11} with respect to WMo_5B_6 and WMo_2B_3 is combined with higher hardness and lower Poisson's ratio of the former three structures compared to the other two. On the phase diagram, the predicted compounds WMo_5B_6 and WMo_2B_3 lie on the straight line connecting WB and α-MoB (Figure 1). Ternary compounds generated by substitutional defects in the crystal structures of binary compounds should have similar mechanical properties (elastic constants, hardness, and fracture toughness). WMo_5B_6 and WMo_2B_3 compositions differ in the ratio Mo:W, and Mo-richer compositions should naturally have structure closer to α-MoB, and vice versa, which will consequently affect the mechanical properties. For WMo_2B_3 and WMo_2B_{11}, which have similar atomic percentages of Mo and W, increasing the atomic percentage of B leads to the transition from the α-MoB-type to the WB_4-type structure, the passage from monoboride to higher boride enormously affects the mechanical properties.

CONCLUSIONS

To predict new ternary W—Mo—B compounds, we used a combination of binary, ternary, and pseudobinary computational searches using the evolutionary algorithm USPEX. Two of the newly found compounds, WMo_2B_3 and WMo_5B_6, have a structural motif of α-MoB, whereas $W_4Mo_4B_{15}$, WMo_2B_{11}, and W_5MoB_{14} have new structure types that have not been observed in binary compounds but can be derived from them by imposing ordered substitutions and ordered vacancies. The quasiharmonic phonon calculations show that WMo_5B_6 and WMo_2B_{11} can be thermodynamically stable at temperatures up to 2000 K, while the formation of WB—MoB solid solutions is likely at high temperatures due to high configurational entropy. The detailed study of electron delocalization in the predicted structures shows its correlation with the mechanical properties (hardness and Poisson's ratio) and with the chemical composition. Ternary systems show the opportunity to discover new hard ternary compounds and high-entropy alloys.

ASSOCIATED CONTENT

Ⓢ Supporting Information

The Supporting Information is available free of charge at https://pubs.acs.org/doi/10.1021/acs.chemmater.0c02440.

Crystal data of predicted compounds, crystal structure details of new compounds, phonon densities of states, electronic densities of states, and data about the configurational entropies of the predicted phases (PDF)

AUTHOR INFORMATION

Corresponding Authors

Alexander G. Kvashnin − *Skolkovo Institute of Science and Technology, Moscow 121025, Russian Federation;* ⓞ orcid.org/0000-0002-0718-6691

Christian Tantardini − *Skolkovo Institute of Science and Technology, Moscow 121025, Russian Federation; Institute of Solid State Chemistry and Mechanochemistry SB RAS, 630128 Novosibirsk, Russian Federation; Linköping University, SE-581 83 Linköping, Sweden;* ⓞ orcid.org/0000-0002-2412-9859

Authors

Hayk A. Zakaryan − *Yerevan State University, Yerevan 0025, Armenia*

Yulia A. Kvashnina − *Pirogov Russian National Research Medical University, Moscow 117997, Russian Federation*

Artem R. Oganov − *Skolkovo Institute of Science and Technology, Moscow 121025, Russian Federation;* ⓞ orcid.org/0000-0001-7082-9728

Complete contact information is available at:
https://pubs.acs.org/10.1021/acs.chemmater.0c02440

Notes

The authors declare no competing financial interest.

REFERENCES

(1) Oganov, A. R.; Pickard, C. J.; Zhu, Q.; Needs, R. J. Structure Prediction Drives Materials Discovery. *Nat. Rev. Mater.* **2019**, *4*, 331−348.

(2) Oganov, A. R.; Glass, C. W. Crystal Structure Prediction Using Ab Initio Evolutionary Techniques: Principles and Applications. *J. Chem. Phys.* **2006**, *124*, 244704.

(3) Oganov, A. R.; Lyakhov, A. O.; Valle, M. How Evolutionary Crystal Structure Prediction Works—and Why. *Acc. Chem. Res.* **2011**, *44*, 227−237.

(4) Lyakhov, A. O.; Oganov, A. R.; Stokes, H. T.; Zhu, Q. New Developments in Evolutionary Structure Prediction Algorithm USPEX. *Comput. Phys. Commun.* **2013**, *184*, 1172−1182.

(5) Wang, Y.; Lv, J.; Zhu, L.; Ma, Y. CALYPSO: A Method for Crystal Structure Prediction. *Comput. Phys. Commun.* **2012**, *183* (10), 2063−2070.

(6) Pickard, C. J.; Needs, R. J. High-Pressure Phases of Silane. *Phys. Rev. Lett.* **2006**, *97* (4), 045504.

(7) Pickard, C. J.; Needs, R. J. Ab Initiorandom Structure Searching. *J. Phys.: Condens. Matter* **2011**, *23* (5), 053201.

(8) Lonie, D. C.; Zurek, E. XtalOpt Version R7: An Open-Source Evolutionary Algorithm for Crystal Structure Prediction. *Comput. Phys. Commun.* **2011**, *182* (10), 2305−2306.

(9) Allahyari, Z.; Oganov, A. R. Multi-Objective Optimization as a Tool for Material Design. In *Handbook of Materials Modeling: Applications: Current and Emerging Materials*; Andreoni, W., Yip, S., Eds.; Springer International Publishing: Cham, 2018; pp 1−15; DOI: 10.1007/978-3-319-50257-1_71-1.

(10) Solozhenko, V. L.; Dub, S. N.; Novikov, N. V. Mechanical Properties of Cubic BC2N, a New Superhard Phase. *Diamond Relat. Mater.* **2001**, *10* (12), 2228−2231.

(11) Solozhenko, V. L.; Gregoryanz, E. Synthesis of Superhard Materials. *Mater. Mater. Today* **2005**, *8* (11), 44−51.

(12) Solozhenko, V. L.; Kurakevych, O. O.; Andrault, D.; Le Godec, Y.; Mezouar, M. Ultimate Metastable Solubility of Boron in Diamond:

Synthesis of Superhard Diamondlike BC5. *Phys. Rev. Lett.* **2009**, *102* (1), 015506.

(13) Akopov, G.; Pangilinan, L. E.; Mohammadi, R.; Kaner, R. B. Perspective: Superhard Metal Borides: A Look Forward. *APL Mater.* **2018**, *6* (7), 070901.

(14) Kvashnin, A. G.; Zakaryan, H. A.; Zhao, C.; Duan, Y.; Kvashnina, Y. A.; Xie, C.; Dong, H.; Oganov, A. R. New Tungsten Borides, Their Stability and Outstanding Mechanical Properties. *J. Phys. Chem. Lett.* **2018**, *9* (12), 3470−3477.

(15) Zhao, C.; Duan, Y.; Gao, J.; Liu, W.; Dong, H.; Dong, H.; Zhang, D.; Oganov, A. R. Unexpected Stable Phases of Tungsten Borides. *Phys. Chem. Chem. Phys.* **2018**, *20* (38), 24665−24670.

(16) Kvashnin, A. G.; Oganov, A. R.; Samtsevich, A. I.; Allahyari, Z. Computational Search for Novel Hard Chromium-Based Materials. *J. Phys. Chem. Lett.* **2017**, *8* (4), 755−764.

(17) Kvashnin, A. G.; Allahyari, Z.; Oganov, A. R. Computational Discovery of Hard and Superhard Materials. *J. Appl. Phys.* **2019**, *126* (4), 040901.

(18) Xie, C.; Zhang, Q.; Zakaryan, H. A.; Wan, H.; Liu, N.; Kvashnin, A. G.; Oganov, A. R. Stable and Hard Hafnium Borides: A First-Principles Study. *J. Appl. Phys.* **2019**, *125* (20), 205109.

(19) Xia, K.; Gao, H.; Liu, C.; Yuan, J.; Sun, J.; Wang, H.-T.; Xing, D. A Novel Superhard Tungsten Nitride Predicted by Machine-Learning Accelerated Crystal Structure Search. *Sci. Bull.* **2018**, *63* (13), 817−824.

(20) Balasubramanian, K.; Khare, S.; Gall, D. Vacancy-Induced Mechanical Stabilization of Cubic Tungsten Nitride. *Phys. Rev. B: Condens. Matter Mater. Phys.* **2016**, *94* (17), 174111.

(21) Zhao, Z.; Bao, K.; Duan, D.; Tian, F.; Huang, Y.; Yu, H.; Liu, Y.; Liu, B.; Cui, T. The Low Coordination Number of Nitrogen in Hard Tungsten Nitrides: A First-Principles Study. *Phys. Chem. Chem. Phys.* **2015**, *17* (20), 13397−13402.

(22) Wang, H.; Li, Q.; Li, Y.; Xu, Y.; Cui, T.; Oganov, A. R.; Ma, Y. Ultra-Incompressible Phases of Tungsten Dinitride Predicted from First Principles. *Phys. Rev. B: Condens. Matter Mater. Phys.* **2009**, *79* (13), 132109.

(23) Zhang, M.; Wang, H.; Wang, H.; Cui, T.; Ma, Y. Structural Modifications and Mechanical Properties of Molybdenum Borides from First Principles. *J. Phys. Chem. C* **2010**, *114* (14), 6722−6725.

(24) Zhao, Z.; Bao, K.; Li, D.; Duan, D.; Tian, F.; Jin, X.; Chen, C.; Huang, X.; Liu, B.; Cui, T. Nitrogen Concentration Driving the Hardness of Rhenium Nitrides. *Sci. Rep.* **2015**, *4* (1), 1−7.

(25) Cheng, X.-Y.; Chen, X.-Q.; Li, D.-Z.; Li, Y.-Y. Computational Materials Discovery: The Case of the W−B System. *Acta Crystallogr., Sect. C: Struct. Chem.* **2014**, *70* (2), 85−103.

(26) Rybkovskiy, D. V.; Kvashnin, A. G.; Kvashnina, Y. A.; Oganov, A. R. Structure, Stability and Mechanical Properties of Boron-Rich Mo−B Phases: A Computational Study. *J. Phys. Chem. Lett.* **2020**, *11* (7), 2393−2401.

(27) Kvashnin, A. G.; Samtsevich, A. I. Phase Transitions in Tungsten Monoborides. *JETP Lett.* **2020**, *111* (6), 343−349.

(28) Lech, A. T.; Turner, C. L.; Lei, J.; Mohammadi, R.; Tolbert, S. H.; Kaner, R. B. Superhard Rhenium/Tungsten Diboride Solid Solutions. *J. Am. Chem. Soc.* **2016**, *138* (43), 14398−14408.

(29) Mohammadi, R.; Turner, C. L.; Xie, M.; Yeung, M. T.; Lech, A. T.; Tolbert, S. H.; Kaner, R. B. Enhancing the Hardness of Superhard Transition-Metal Borides: Molybdenum-Doped Tungsten Tetraboride. *Chem. Mater.* **2016**, *28* (2), 632−637.

(30) Mohammadi, R.; Xie, M.; Lech, A. T.; Turner, C. L.; Kavner, A.; Tolbert, S. H.; Kaner, R. B. Toward Inexpensive Superhard Materials: Tungsten Tetraboride-Based Solid Solutions. *J. Am. Chem. Soc.* **2012**, *134* (51), 20660−20668.

(31) Hebbache, M.; Stuparević, L.; Živković, D. A New Superhard Material: Osmium Diboride OsB2. *Solid State Commun.* **2006**, *139* (5), 227−231.

(32) Pangilinan, L. E.; Turner, C. L.; Akopov, G.; Anderson, M.; Mohammadi, R.; Kaner, R. B. Superhard Tungsten Diboride-Based Solid Solutions. *Inorg. Chem.* **2018**, *57* (24), 15305−15313.

(33) Kvashnin, A. G.; Rybkovskiy, D. V.; Filonenko, V. P.; Bugakov, V. I.; Zibrov, I. P.; Brazhkin, V. V.; Oganov, A. R.; Osiptsov, A. A.; Zakirov, A. Ya. WB5−x: Synthesis, Properties, and Crystal Structure. New Insights Into the Long-Debated Compound. *Adv. Sci.* **2020**, 2000775.

(34) Xie, M.; Mohammadi, R.; Mao, Z.; Armentrout, M. M.; Kavner, A.; Kaner, R. B.; Tolbert, S. H. Exploring the High-Pressure Behavior of Superhard Tungsten Tetraboride. *Phys. Rev. B: Condens. Matter Mater. Phys.* **2012**, *85* (6), 064118.

(35) Mohammadi, R.; Lech, A. T.; Xie, M.; Weaver, B. E.; Yeung, M. T.; Tolbert, S. H.; Kaner, R. B. Tungsten Tetraboride, an Inexpensive Superhard. *Proc. Natl. Acad. Sci. U. S. A.* **2011**, *108* (27), 10958−10962.

(36) Bushlanov, P. V.; Blatov, V. A.; Oganov, A. R. Topology-Based Crystal Structure Generator. *Comput. Phys. Commun.* **2019**, *236*, 1−7.

(37) Perdew, J. P. Density-Functional Approximation for the Correlation Energy of the Inhomogeneous Electron Gas. *Phys. Rev. B: Condens. Matter Mater. Phys.* **1986**, *33*, 8822.

(38) Kresse, G.; Joubert, D. From Ultrasoft Pseudopotentials to the Projector Augmented-Wave Method. *Phys. Rev. B: Condens. Matter Mater. Phys.* **1999**, *59* (3), 1758−1775.

(39) Kresse, G.; Hafner, J. Ab Initio Molecular Dynamics for Liquid Metals. *Phys. Rev. B: Condens. Matter Mater. Phys.* **1993**, *47*, 558−561.

(40) Kresse, G.; Furthmüller, J. Efficiency of Ab-Initio Total Energy Calculations for Metals and Semiconductors Using a Plane-Wave Basis Set. *Comput. Mater. Sci.* **1996**, *6*, 15−50.

(41) Kresse, G.; Furthmüller, J. Efficient Iterative Schemes for Ab Initio Total-Energy Calculations Using a Plane-Wave Basis Set. *Phys. Rev. B: Condens. Matter Mater. Phys.* **1996**, *54*, 11169−11186.

(42) Methfessel, M.; Paxton, A. T. High-Precision Sampling for Brillouin-Zone Integration in Metals. *Phys. Rev. B: Condens. Matter Mater. Phys.* **1989**, *40* (6), 3616−3621.

(43) Momma, K.; Izumi, F. VESTA 3 for Three-Dimensional Visualization of Crystal, Volumetric and Morphology Data. *J. Appl. Crystallogr.* **2011**, *44*, 1272−1276.

(44) Kern, G.; Kresse, G.; Hafner, J. Ab Initio Calculation of the Lattice Dynamics and Phase Diagram of Boron Nitride. *Phys. Rev. B: Condens. Matter Mater. Phys.* **1999**, *59*, 8551−8559.

(45) Togo, A.; Tanaka, I. First Principles Phonon Calculations in Materials Science. *Scr. Mater.* **2015**, *108*, 1−5.

(46) Togo, A.; Oba, F.; Tanaka, I. First-Principles Calculations of the Ferroelastic Transition between Rutile-Type and CaCl2-Type SiO2 at High Pressures. *Phys. Rev. B: Condens. Matter Mater. Phys.* **2008**, *78*, 134106.

(47) Kresse, G.; Hafner, J. Ab Initio Molecular Dynamics for Liquid Metals. *Phys. Rev. B: Condens. Matter Mater. Phys.* **1993**, *47* (1), 558−561.

(48) Kresse, G.; Hafner, J. Ab Initio Molecular-Dynamics Simulation of the Liquid-Metal-Amorphous-Semiconductor Transition in Germanium. *Phys. Rev. B: Condens. Matter Mater. Phys.* **1994**, *49* (20), 14251−14269.

(49) Kresse, G.; Furthmüller, J. Efficient Iterative Schemes for Ab Initio Total-Energy Calculations Using a Plane-Wave Basis Set. *Phys. Rev. B: Condens. Matter Mater. Phys.* **1996**, *54* (16), 11169−11186.

(50) Mazhnik, E.; Oganov, A. R. A Model of Hardness and Fracture Toughness of Solids. *J. Appl. Phys.* **2019**, *126* (12), 125109.

(51) Andrievski, R. A. Superhard Materials Based on Nanostructured High-Melting Point Compounds: Achievements and Perspectives. *Int. J. Refract. Hard Met.* **2001**, *19* (4), 447−452.

(52) Stone, D. S.; Yoder, K. B.; Sproul, W. D. Hardness and Elastic Modulus of TiN Based on Continuous Indentation Technique and New Correlation. *J. Vac. Sci. Technol., A* **1991**, *9* (4), 2543−2547.

(53) Westbrook, J. H.; Conrad, H. *The Science of Hardness Testing and Its Research Applications*; American Society for Metals: Cleveland, OH, 1973.

(54) Steinitz, R.; Binder, I.; Moskowitz, D. System Molybdenum-Boron and Some Properties of The Molybdenum-Borides. *JOM* **1952**, *4* (9), 983−987.

(55) Oganov, A. R.; Chen, J.; Gatti, C.; Ma, Y.; Ma, Y.; Glass, C. W.; Liu, Z.; Yu, T.; Kurakevych, O. O.; Solozhenko, V. L. Ionic High-Pressure Form of Elemental Boron. *Nature* **2009**, *457* (7231), 863−867.

(56) van Setten, M. J.; Uijttewaal, M. A.; de Wijs, G. A.; de Groot, R. A. Thermodynamic Stability of Boron: The Role of Defects and Zero Point Motion. *J. Am. Chem. Soc.* **2007**, *129* (9), 2458−2465.

(57) Brazhkin, V. V.; Taniguichi, T.; Akaishi, M.; Popova, S. V. Fabrication of β-Boron by Chemical-Reaction and Melt-Quenching Methods at High Pressures. *J. Mater. Res.* **2004**, *19* (6), 1643−1648.

(58) Ogitsu, T.; Schwegler, E.; Galli, G. β-Rhombohedral Boron: At the Crossroads of the Chemistry of Boron and the Physics of Frustration. *Chem. Rev.* **2013**, *113* (5), 3425−3449.

(59) Masago, A.; Shirai, K.; Katayama-Yoshida, H. Crystal Stability of Alpha- and Beta-Boron. *Phys. Rev. B: Condens. Matter Mater. Phys.* **2006**, *73* (10), 104102.

(60) Widom, M.; Mihalkovič, M. Relative Stability of α and β Boron. *J. Phys. Conf. Ser.* **2009**, *176*, 012024.

(61) Ogitsu, T.; Gygi, F.; Reed, J.; Motome, Y.; Schwegler, E.; Galli, G. Imperfect Crystal and Unusual Semiconductor: Boron, a Frustrated Element. *J. Am. Chem. Soc.* **2009**, *131* (5), 1903−1909.

(62) Ogitsu, T.; Gygi, F.; Reed, J.; Udagawa, M.; Motome, Y.; Schwegler, E.; Galli, G. Geometrical Frustration in an Elemental Solid: An Ising Model to Explain the Defect Structure of $\ensuremath{\beta}$-Rhombohedral Boron. *Phys. Rev. B: Condens. Matter Mater. Phys.* **2010**, *81* (2), 020102.

(63) Tang, H.; Gao, X.; Zhang, J.; Gao, B.; Zhou, W.; Yan, B.; Li, X.; Zhang, Q.; Peng, S.; Huang, D.; Zhang, L.; Yuan, X.; Wan, B.; Peng, C.; Wu, L.; Zhang, D.; Liu, H.; Gu, L.; Gao, F.; Irifune, T.; Ahuja, R.; Mao, H.-K.; Gou, H. Boron-Rich Molybdenum Boride with Unusual Short-Range Vacancy Ordering, Anisotropic Hardness, and Super-conductivity. *Chem. Mater.* **2020**, *32* (1), 459−467.

(64) Tantardini, C.; Benassi, E. Crystal Structure Resolution of an Insulator Due to the Cooperative Jahn−Teller Effect through Bader's Theory: The Challenging Case of Cobaltite Oxide Y114. *Dalton Trans* **2018**, *47* (15), 5483−5491.

(65) Okada, S.; Atoda, T.; Higashi, I.; Takahashi, Y. Preparation of Single Crystals of MoB2 by the Aluminium-Flux Technique and Some of Their Properties. *J. Mater. Sci.* **1987**, *22* (8), 2993−2999.

(66) Okada, S.; Kudou, K.; Lundström, T. Preparations and Some Properties of W2B, δ-WB and WB2 Crystals from High-Temperature Metal Solutions. *Jpn. J. Appl. Phys.* **1995**, *34* (1R), 226.